

Truncated hexa-octahedral magnetite crystals in ALH84001: Presumptive biosignatures

Kathie L. Thomas-Keprta^{*†}, Simon J. Clemett^{*}, Dennis A. Bazylinski[‡], Joseph L. Kirschvink[§], David S. McKay[¶], Susan J. Wentworth^{*}, Hojatollah Vali^{||}, Everett K. Gibson, Jr.^{**}, Mary Fae McKay^{††}, and Christopher S. Romanek^{††}

^{*}Lockheed Martin, 2400 NASA Road 1, Mail Code C23, Houston, TX 77058; [†]Iowa State University, Department of Microbiology, 207 Science I, Ames, IA 50011; [‡]California Institute of Technology, Division of Geological and Planetary Sciences, 1200 East California Boulevard, Pasadena, CA 91125; National Aeronautics and Space Administration/Johnson Space Center, [¶]Mail Code SN, ^{**}Mail Code SN2, ^{††}Mail Code SL, Houston, TX 77058; ^{||}McGill University, Department of Earth and Planetary Sciences, 3450 University Street, Montreal, PQ H3A 2A7, Canada; and ^{††}Savannah River Ecology Laboratory, Drawer E, University of Georgia, Aiken, SC 29802

Edited by Bruce Watson, Rensselaer Polytechnic Institute, Troy, NY, and approved December 18, 2000 (received for review October 22, 2000)

McKay et al. [(1996) *Science* 273, 924–930] suggested that carbonate globules in the meteorite ALH84001 contained the fossil remains of Martian microbes. We have characterized a subpopulation of magnetite (Fe₃O₄) crystals present in abundance within the Fe-rich rims of these carbonate globules. We find these Martian magnetites to be both chemically and physically identical to terrestrial, biogenically precipitated, intracellular magnetites produced by magnetotactic bacteria strain MV-1. Specifically, both magnetite populations are single-domain and chemically pure, and exhibit a unique crystal habit we describe as truncated hexa-octahedral. There are no known reports of inorganic processes to explain the observation of truncated hexa-octahedral magnetites in a terrestrial sample. In bacteria strain MV-1 their presence is therefore likely a product of Natural Selection. Unless there is an unknown and unexplained inorganic process on Mars that is conspicuously absent on the Earth and forms truncated hexa-octahedral magnetites, we suggest that these magnetite crystals in the Martian meteorite ALH84001 were likely produced by a biogenic process. As such, these crystals are interpreted as Martian magnetofossils and constitute evidence of the oldest life yet found.

We report here the presence of single-domain, chemically pure, truncated hexa-octahedral magnetite crystals in terrestrial samples and Martian meteorite ALH84001. We suggest that the truncated hexa-octahedral magnetite crystals in the Martian meteorite ALH84001 were likely formed by a biogenic process. These magnetite crystals are embedded in $\approx 3.91 (\pm 0.05)$ -Ga-old carbonate globules (1) that fill cracks and pore space in the 4.5-Ga-old Martian meteorite ALH84001. These truncated hexa-octahedral magnetite crystals are identical to those produced intracellularly by the marine magnetotactic bacterium strain MV-1 (2–7); natural selection has optimized the magnetic moment of MV-1 magnetite particles (2, 8–12). There is no known natural terrestrial inorganic mechanism that can explain the observation of truncated hexa-octahedral magnetite crystals associated with MV-1. Therefore, unless there is an unknown inorganic process on Mars, which seems to be absent on the Earth, we suggest that ALH84001 truncated hexa-octahedral magnetites formed by a similar mechanism to their terrestrial biogenic counterparts. As such, these crystals are interpreted as Martian magnetofossils and they constitute evidence of the oldest life yet found. In support of this, we note that early Mars likely had free-standing bodies of liquid water (13, 14), and both organic (15) and inorganic carbon and energy (e.g., atmospheric CO₂¹³) sources. Furthermore, early Mars also likely possessed a substantial planetary magnetic field (16), which would have been sufficient to support the evolution and growth of magnetotactic bacteria.

Characteristics of Biogenic Magnetite

Magnetotactic bacteria produce well ordered membrane-bounded intracellular crystals of magnetite (Fe₃O₄) and/or

greigite (Fe₃S₄) called “magnetosomes.” They are generally arranged in chains parallel to the long axis of the cell. The torque induced by the Earth’s magnetic field on these chains overwhelms thermal agitation, allowing the bacteria to align passively along the Earth’s geomagnetic field lines like a compass needle (8, 9). Coupled with flagellar motility, aerotaxis, and magnetotaxis, this allows these bacteria to locate and maintain an optimal position in vertical chemical gradients in aquatic environments (4). Magnetotactic bacteria exert strict genetic control over the composition, size, morphology, and crystallographic orientation of their biogenic magnetite to maximize their cellular magnetic moment (2, 10–12). Physical and chemical controls of the biomineralization processes are achieved by precipitating magnetite and greigite within small intracellular membrane vesicles (17).

The intracellular magnetite crystals produced by magnetotactic bacterium strain MV-1 display six distinctive properties: (i) narrow size-range (i.e., single-domain for uniform magnetization) and shape (restricted width-to-length (W/L) ratios); (ii) chemical purity; (iii) few crystallographic defects; (iv) an unusual truncated hexa-octahedral morphology; (v) elongation along the [111] axis; and (vi) alignment in chains within cells. These characteristics are the result of biochemical and genetic control by the organism and are consistent with natural (Darwinian) selection to maximize the magnetic dipole moment of the individual magnetite crystals as well as that of the entire cell (2). These characteristics can be used to define a terrestrial biosignature (2, 7, 18).

A biosignature is useful only if it is not produced by natural inorganic processes; that is, one that does not happen through random, stochastic interactions or is not a product of directed human intervention, which is better described as a synthetic inorganic process. No published reports of inorganic “MV-1-like” truncated hexa-octahedral magnetites are known. Because the chemical and physical principles that underlie these six criteria are universal, they are not restricted to terrestrial samples but are applicable to Martian samples as well.

Comparison of MV-1 Biogenic Magnetite and ALH84001 Magnetite

Approximately one-fourth of the magnetites observed in Martian meteorite ALH84001 are truncated hexa-octahedral, and share five of the six characteristics that define the MV-1 biosignature:

(i) Both the truncated hexa-octahedral magnetites from ALH84001 and strain MV-1 cluster in the superparamagnetic to single-domain region of the Butler–Banerjee plot for magnetite (2, 3). MV-1 magnetites appear to nucleate within a cell mem-

This paper was submitted directly (Track II) to the PNAS office.

Abbreviation: TEM, transmission electron microscope.

[†]To whom reprint requests should be addressed. E-mail: kthomas@ems.jsc.nasa.gov.

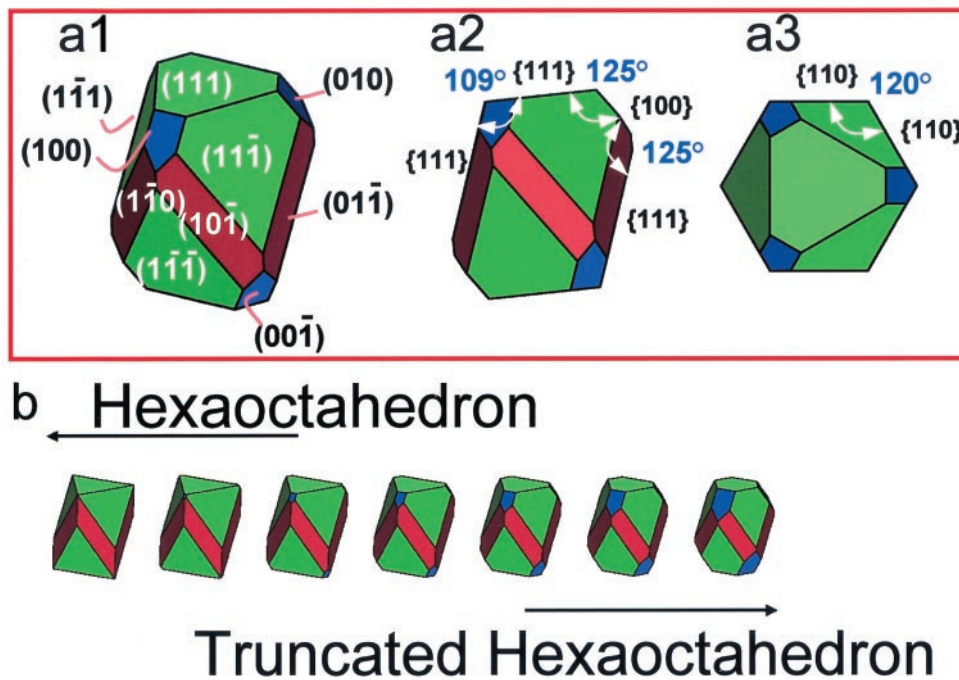


Fig. 1. Idealized truncated hexa-octahedral crystal habit of magnetite from the magnetotactic bacterium strain MV-1. Previous reports describing the MV-1 crystal habit misidentified this type of crystal, defining it as a hexa-octahedron (2, 10). [Note: In the microbiological community these crystals have been referred to as “parallelepiped”(10).] Magnetite with hexa-octahedral crystal habit is elongated along one of the $[111]$ axes, with eight $\{111\}$ octahedral (green) faces and six $\{110\}$ hexagonal (red) faces (see supplemental data, Fig. 4 *b1–b3*). In contrast, magnetite with truncated hexa-octahedral crystal habit has eight $\{111\}$ octahedral faces, six $\{110\}$ hexagonal faces, and six $\{100\}$ cubic (blue) faces. The two $\{111\}$ faces perpendicular to the axis of elongation are equivalent to each other but not to the remaining six $\{111\}$ faces that are not parallel to the elongation axis. Other biogenic magnetite geometries reported in the literature include elongated cubo-octahedrons (in wild-type bacteria), hexa-octahedrons (in vibroid bacteria), and hexa-octahedrons (in cocci) (for a complete discussion see ref. 10 and supplemental data, Fig. 4). (a1) Orthographic projection of a truncated hexa-octahedron. (a2) Truncated hexa-octahedron viewed down the $[1\bar{1}0]$ zone axis. (a3) Truncated hexa-octahedron viewed down the $[111]$ zone axis. (b) The transition from hexa-octahedral to truncated hexa-octahedral crystal habit is achieved by adding cubic $\{100\}$ faces (blue surfaces). The degree of truncation appears variable in MV-1 and ALH84001 magnetites, with hexa-octahedral crystal habit being one end member (far left) of the progression shown here.

brane (17) and grow from the superparamagnetic into the single-domain size range (i.e., they behave as perfect bar magnets) with well defined shape anisotropies and a narrow, asymmetric width-to-length (W/L) distribution. In the case of MV-1 magnetites, these characteristics arise from natural selection, as superparamagnetic and multidomain crystals are of no value for magnetotaxis (18). ALH84001 truncated hexa-octahedral magnetites display identical characteristics.

(ii) Both populations of magnetite crystals are chemically pure, containing only Fe and O at detectable levels (>150 ppm) (2). Bacterial Fe-acquisition (siderophore) systems are generally specific for their uptake of Fe (19), although this depends on the relative availability of Fe relative to other elements that can be complexed by the siderophore. Such chemical specificity is typical of bacterial pathways for Fe acquisition and transport, which involve multiple chelation and redox steps linked with adenosine triphosphate-coupled transport across lipid-bilayer membranes (20). Although MV-1 is routinely cultured in a growth medium containing Cu, Co, Zn, Mo, Ni, Mg, Al, and Mn (4), these elements, common as impurities in inorganic magnetite, are not detected in biogenic magnetite.

(iii) MV-1 magnetites have few crystallographic defects that act to attenuate the crystal’s ferromagnetic properties, whereas ALH84001 truncated hexa-octahedral magnetites were defect free. In the case of MV-1 magnetite, the occasional twin in the $\{111\}$ plane (5, 6) has no effect on the magnetic properties because the unpaired Bohr magnetons in the crystal remain aligned perpendicular to the twin plane. The lack of lattice

defects acts to optimize the net magnetic moment of the magnetite crystal. Consequently, the ability to grow defect-free crystals is also likely a product of natural selection.

(iv) Both populations of magnetite are characterized by having a specific crystal habit. We have previously described this crystal habit as elongated prismatic (a term that should be avoided in the future because it is inconsistent with actual morphology) or hexa-octahedral, emphasizing that the crystal has six $\{110\}$ hexagonal faces⁵⁵ and eight $\{111\}$ octahedral faces (ref. 2; George W. Hart, personal communication). On further transmission electron microscope (TEM) analyses we now suggest that the term hexa-octahedron does not strictly describe the habit of either MV-1 or ALH84001 magnetite crystals (see Fig. 4, which is published as supplemental data on the PNAS web site, www.pnas.org). Rather, we suggest that the crystal habit can now better be described as a *truncated* hexa-octahedron (George W. Hart, personal communication). This modified crystal habit has not previously been recognized for MV-1 biogenic magnetite (ref. 10; Fig. 1). Analyses of multiple individual MV-1 crystals indicate that the degree of truncation (i.e., the size of the $\{100\}$ faces) of the hexa-octahedral MV-1 magnetite is variable between crystals (Fig. 1*b*). We have verified this truncated hexa-octahedral habit by rotating magnetites $\pm 45^\circ$ in a TEM so as to

⁵⁵We note that the $\{110\}$ form is a dodecahedron; however, in the context discussed here only six of the possible twelve $\{110\}$ faces are expressed. So we describe these six faces as “hexa-octahedral,” even though this is not strictly correct in a crystallographic context.

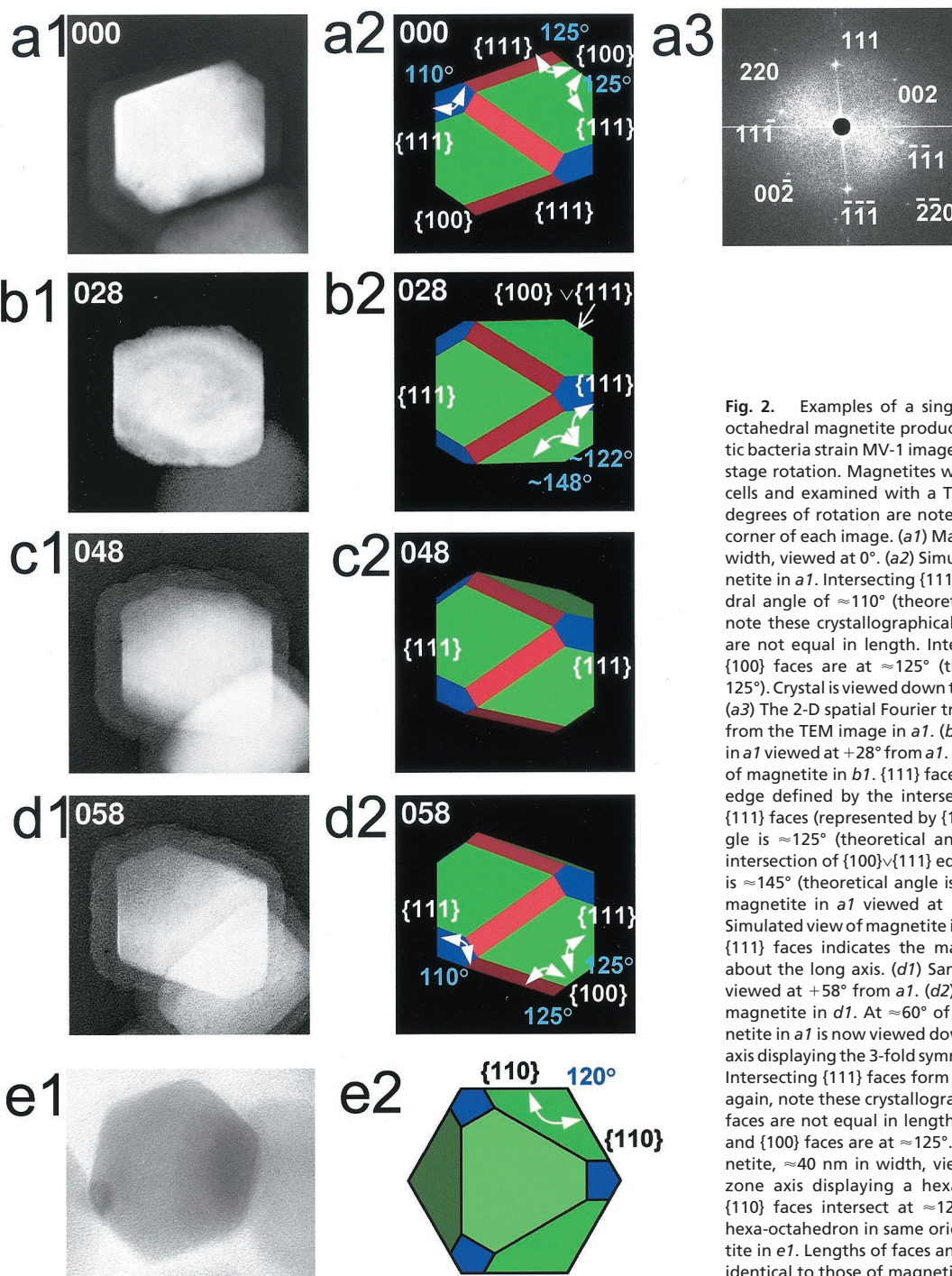


Fig. 2. Examples of a single truncated hexa-octahedral magnetite produced by magnetotactic bacteria strain MV-1 imaged with incremental stage rotation. Magnetites were extracted from cells and examined with a TEM at 200 kV. The degrees of rotation are noted in the upper left corner of each image. (a1) Magnetite, ≈ 35 nm in width, viewed at 0° . (a2) Simulated view of magnetite in a1. Intersecting $\{111\}$ faces form a dihedral angle of $\approx 110^\circ$ (theoretical angle is 109°); note these crystallographically equivalent faces are not equal in length. Intersecting $\{111\}$ and $\{100\}$ faces are at $\approx 125^\circ$ (theoretical angle is 125°). Crystal is viewed down the $[1-10]$ zone axis. (a3) The 2-D spatial Fourier transform calculated from the TEM image in a1. (b1) Same magnetite in a1 viewed at $+28^\circ$ from a1. (b2) Simulated view of magnetite in b1. $\{111\}$ faces are bound by the edge defined by the intersection of $\{100\}$ and $\{111\}$ faces (represented by $\{100\} \vee \{111\}$); this angle is $\approx 125^\circ$ (theoretical angle is $\approx 122^\circ$). The intersection of $\{100\} \vee \{111\}$ edge and a $\{110\}$ face is $\approx 145^\circ$ (theoretical angle is $\approx 148^\circ$). (c1) Same magnetite in a1 viewed at $+48^\circ$ from a1. (c2) Simulated view of magnetite in c1. Position of the $\{111\}$ faces indicates the magnetite is rotated about the long axis. (d1) Same magnetite in a1 viewed at $+58^\circ$ from a1. (d2) Simulated view of magnetite in d1. At $\approx 60^\circ$ of rotation, the magnetite in a1 is now viewed down the $[-101]$ zone axis displaying the 3-fold symmetry of this crystal. Intersecting $\{111\}$ faces form an angle of $\approx 110^\circ$; again, note these crystallographically equivalent faces are not equal in length. Intersecting $\{111\}$ and $\{100\}$ faces are at $\approx 125^\circ$. (e1) Another magnetite, ≈ 40 nm in width, viewed down a $[111]$ zone axis displaying a hexagonal projection. $\{110\}$ faces intersect at $\approx 120^\circ$. (e2) Truncated hexa-octahedron in same orientation as magnetite in e1. Lengths of faces and angles are nearly identical to those of magnetite in e1.

view multiple 2-D projections, from which the 3-D geometry can be determined. For example, the single MV-1 magnetite crystal in Fig. 2, is shown viewed at four rotation angles spanning $\approx 60^\circ$ (Fig. 2). The 3-fold symmetry and presence of $\{100\}$ faces is indicative of the truncated hexa-octahedral habit (Fig. 2). Elongated ALH84001 magnetites also show this habit (Fig. 3). Additional images of MV-1 and ALH84001 truncated hexa-octahedral magnetites in identical orientations are shown in supplemental data, Fig. 5.

(v) Both populations of magnetite crystals are elongated along the zone axis $[111]$ (Figs. 2 and 3). This elongation increases the magnetic stability of the crystal (the microscopic coercivity) by

aligning the directions of the minimum magnetocrystalline and shape anisotropy energies and enlarging the single-domain stability field (5, 7).

(vi) MV-1 magnetite crystals are aligned in chains within living cells. In this configuration the magnetic dipole moment of the cell is maximized because the overall magnetic moment of the cell is the sum of the dipole moments of the individual magnetite crystals. When the organism dies the magnetosome membrane decomposes, and the chain collapses to dissipate the magnetostatic potential energy. Thus, biogenic magnetites from dead organisms embedded in both contemporary and ancient samples rarely show evidence of their former arrangement in chains (7,

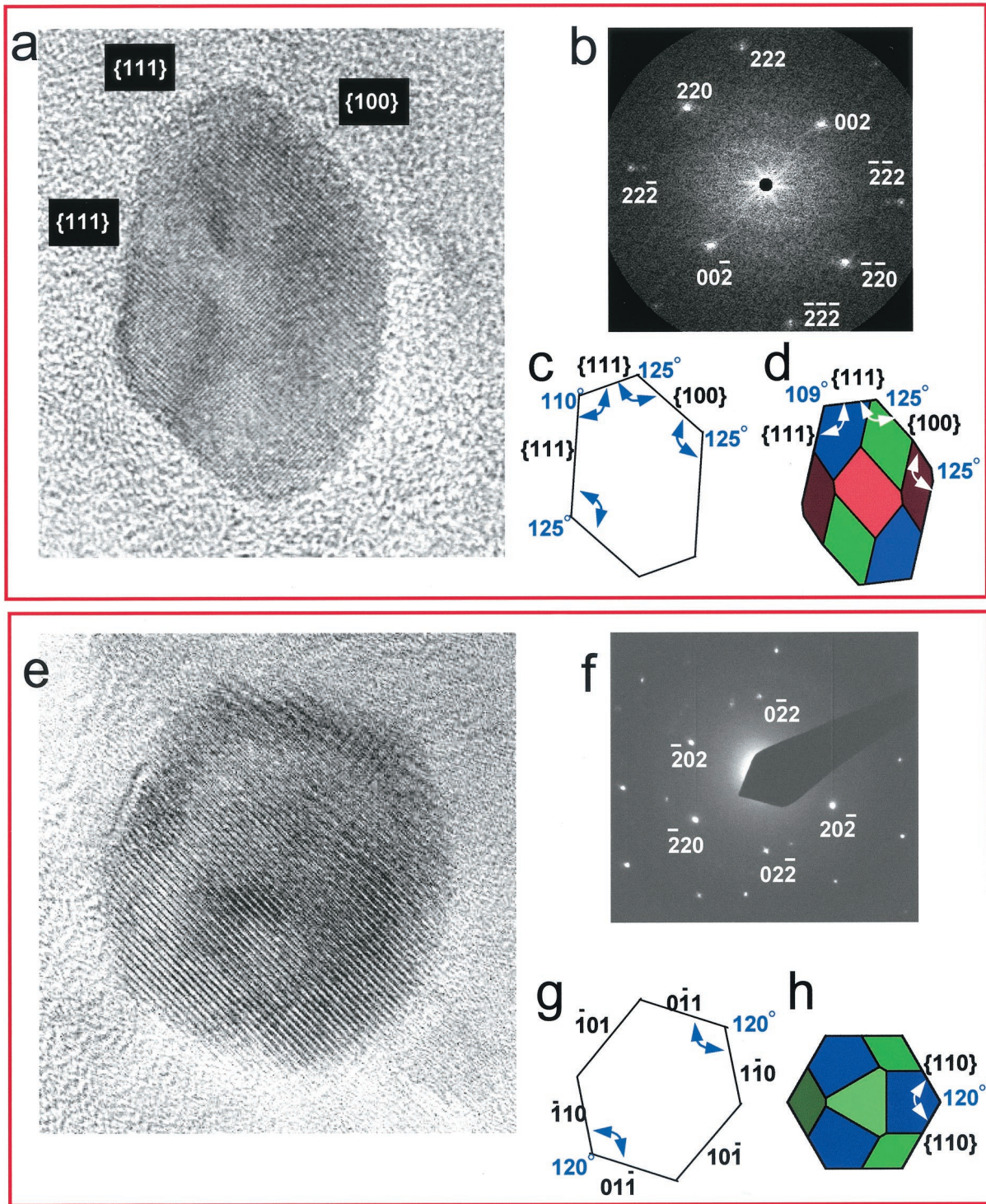


Fig. 3. (a) High-resolution TEM image of a single hexa-octahedral magnetite particle ($\approx 35 \times 25$ nm) embedded in carbonate from Martian meteorite ALH84001. The carbonate matrix surrounding the magnetite is fine-grained, lacks long-range order, and shows no other recognizable structures (such as vesicular structure that would be expected by thermal decomposition of FeCO_3 to Fe_3O_4). The crystal is aligned down the $[1-10]$ zone axis and is elongated parallel to the $[111]$ axis. (b) The 2-D spatial Fourier transform calculated from the TEM image shown in (a). (c) Outline of magnetite in a shows the $\{111\}$ faces intersect at $\approx 110^\circ$ (theoretical angle is 109°); $\{100\}$ faces intersect $\{111\}$ faces at $\approx 125^\circ$ (theoretical angle is 125°). (d) The crystal habit we suggest for Martian magnetite (a) is the truncated hexa-octahedron that has a crystal habit identical to that described for biogenic magnetite crystals produced by strain MV-1 (see Fig. 2). The $\{100\}$ blue faces are larger than those previously shown for the MV-1 magnetite consistent with variation in the degree of cubic faceting (also see Fig. 1b). None of the geometries of elongated biogenic magnetites in supplemental Fig. 4 adequately describes that of the ALH84001 magnetite in a. (e) High-resolution image of same crystal in a rotated 90° and viewed down the $[111]$ zone axis. (f) Electron diffraction pattern of the TEM image shown in e. (g) Outline of magnetite in e shows the $\{110\}$ faces intersect at $\approx 120^\circ$ (theoretical angle is 120°). (h) Simulated truncated hexa-octahedron viewed down the $[111]$ axis, same orientation as magnetite in e.

18). Chains of truncated hexa-octahedral magnetites have not been observed by us in ALH84001.

In summary, truncated hexa-octahedral magnetites in ALH84001 carbonate globules are chemically and physically indistinguishable from those produced by bacterial strain MV-1 (with the exception of chains that, as noted above, are rarely observed after cell death). Thus, we conclude that a biogenic process is the most plausible explanation, when considering all of the available data^{††} for the formation of the Martian truncated hexa-octahedral magnetite crystals.

Other magnetites in ALH84001 are chemically and physically distinct from the truncated hexa-octahedral magnetites (matching at most only one or two of the six criteria outlined above). These magnetites are analogous to some inorganic magnetites observed in terrestrial samples. In this regard, we note that intimate mixtures of both biogenic and abiotic magnetite crystals (ref. 2 and references therein) are observed in samples of recent and ancient terrestrial carbonates.

Survivability of Magnetotactic Bacteria on Mars

Would the environment on early Mars have favored the survival of magnetotactic bacteria? All terrestrial life requires liquid water, a carbon source, and a source of energy. In addition, magnetotaxis requires a permanent magnetic field. These requirements are discussed below, in the context of early Mars.

Liquid Water. Surface features suggest that early Mars had significant quantities of standing water on its surface (i.e., oceans and lakes) during the first two Ga (13). Recent surface features (<1 Ma) suggest that liquid water may have flowed out of shallow depths and may even still be present near the Martian surface (14). Isotopic D/H ratios in the Martian shergottite QUE94201 (crystallization age of 327 Ma) suggest the abundance of water in the Martian crust at that time was two to three times greater than previously believed (21). Finally, the observation in nearly all Martian meteorites [with crystallization ages from ≈ 4.5 Ga (ALH84001) to ≈ 0.16 Ga (Shergotty)] of secondary mineral phases (22) including phyllosilicates, carbonates, sulfates, and chlorides are interpreted to have formed from aqueous weathering on Mars (23). This provides additional evidence for liquid water in the near-surface of Mars over most of its history.

Sources of Carbon. Terrestrial magnetotactic bacteria can derive energy from the oxidation of organic and/or inorganic compounds. For example, strain MV-1 can grow chemoorganoheterotrophically by the oxidation of organic acids (e.g., succinic acid) and amino acids or chemolithoautotrophically by the oxidation of reduced sulfur (e.g., sulfides) by using CO₂ as its major carbon source (D.A.B., unpublished data). The present-day tenuous Martian atmosphere is rich in CO₂ ($\approx 95\%$) (24). It is unknown whether the early Mars atmosphere was dense and/or CO₂-rich, although this is considered likely because the ancient atmospheres of Earth-like planets were composed primarily of CO₂ and H₂O (13). CO₂ dissolved in groundwater could then be the primary carbon source for autotrophic magnetotactic bacteria. In addition, it is likely that the level of O₂ in

early Martian atmosphere (24) was greater than at present due to dissociation of atmospheric O₂-bearing species (25). These latter findings are particularly significant in that all known terrestrial magnetite-producing magnetotactic bacteria, with one exception, are at least facultative microaerophiles (i.e., they respire with O₂) (11).

Although no organic matter was detected in the four soil samples taken by Viking 1 (landed June 3, 1976) and Viking 2 (landed June 20, 1976) landers when using their onboard gas chromatograph-mass spectrometers (detection limit for toluene ≈ 1 ppb) (26), this is now believed to be the result of photocatalytic oxidation on the Martian surface (27) and/or the formation of benzenecarboxylic acid salts (27). Consequently, the lack of detectable organic compounds at the two Viking sites (Chryse Planitia & Utopia Planitia) may be a surface-limited feature, and organic carbon could exist at deeper levels. Indigenous aromatic organic compounds have been detected in the two Martian meteorites—ALH84001 (15) and Nakhla (S.J.C., unpublished data).

Magnetic Fields. The strength of naturally occurring magnetic interactions on chemical and biological processes is much smaller than the thermal energies kT and, hence, on thermodynamic grounds, chemical and biological processes cannot be influenced by magnetic fields to any measurable degree. Therefore, it is impossible for natural inorganic processes to favor the formation of magnetite crystals optimized with respect to their interaction with a magnetic field. However, Darwinian evolution in biological systems that use magnetotaxis would favor the evolution of magnetites optimized for magnetic field interactions. Field studies of the swimming behavior of terrestrial magnetotactic bacteria argue strongly that magnetotaxis is likely the main driving force in their production of magnetite (4, 5, 7). Although results from the Mars Global Surveyor (MGS) indicate that Mars had a significant global magnetic field until ≈ 4 Ga ago (16), remnant crustal magnetism is nevertheless today both widespread and sufficiently strong ($>5 \mu T$) to support magnetotaxis (16, 18).

In conclusion, early Mars likely had free-standing bodies of water, a CO₂-rich atmosphere containing trace O₂, solar and geothermal energy sources, multiple carbon reservoirs, and a global magnetic field. Such an environment meets all of the requirements necessary for the growth and evolution of microbes using magnetotaxis. These conditions are generally accepted to have persisted for at least several hundred Ma on early Mars.

Truncated hexa-octahedral magnetites in ALH84001 have no known terrestrial abiotic analog. Terrestrial bacteria strain MV-1 produce truncated hexa-octahedral magnetites that appear to have been optimized for magnetotaxis. The Martian truncated hexa-octahedral magnetites and the terrestrial MV-1 biogenic truncated hexa-octahedral magnetites are physically and chemically indistinguishable. Without a credible inorganic process that can account for truncated hexa-octahedral magnetites on Mars *but not on the Earth*, we suggest this is evidence for the earliest form of life known.

We thank J. Hultberg of the National Aeronautics and Space Administration (NASA)/Johnson Space Center Scientific and Technical Information center, R. Christoffersen, T. D. Raub, R. N. Zare, P. R. Buseck, S. Keptra, K. White, R. B. Frankel, and the Honorable T. Campbell. We also thank J. Kulick and A. Jacobson of the Materials Research Science and Engineering Center at the University of Houston. We acknowledge the funding and support of NASA's Astrobiology Institute and the Exobiology Program. D.A.B. was supported by the National Science Foundation.

^{††}We respectfully refer readers to ref. 2 and references therein, which summarize some of the recent literature describing inorganic and biogenic formation mechanisms of sub-micrometer-sized magnetite.

1. Borg, L. E., Connelly, J. N., Nyquist, L. E., Shih, C.-Y., Wisemann, H. & Reese, Y. (1999) *Science* **286**, 90–94.
2. Thomas-Keptra, K. L., Bazylinski, D. A., Kirschvink, J. L., Clemett, S. J., McKay, D. S., Wentworth, S. J., Vali, H., Gibson, E. K., Jr., & Romanek, C. S. (2000) *Geochim. Cosmochim. Acta* **64**, 4049–4081.

3. Butler, R. F. & Banerjee, S. K. (1975) *J. Geophys. Res.* **80**, 4049–4058.
4. Frankel, R. B., Bazylinski, D. A., Johnson, M. S. & Taylor, B. L. (1997) *Biophys. J.* **73**, 994–1000.
5. Vali, H. & Kirschvink, J. L. (1991) in *Iron Biominerals*, eds. Frankel, R. B. & Blakemore, R. P. (Plenum, New York), pp. 97–115.

6. Devouard, B., Posfai, M., Hua, X., Bazylinski, D. A., Frankel, R. B. & Buseck, P. R. (1998) *Am. Mineral.* **83**, 1387–1398.
7. Chang, S.-B. R. & Kirschvink, J. L. (1989) *Annu. Rev. Earth Planet. Sci.* **17**, 169–195.
8. Blakemore, R. P. (1975) *Science* **190**, 377–379.
9. Frankel, R. B., Blakemore, R. P. & Wolfe, R. S. (1979) *Science* **203**, 1355–1356.
10. Mann, S., Sparks, N. H. C. & Wade, V. J. (1991) in *Iron Biominerals*, eds. Frankel, R. B. & Blakemore, R. P. (Plenum, New York), pp. 21–49.
11. Bazylinski, D. A. & Moskowicz, B. M. (1997) in *Geomicrobiology: Interactions between Microbes and Minerals*, eds. Banfield, J. F. & Nealson, K. H. (Mineralogical Society of America, Washington, DC), pp. 181–223.
12. Sparks, N. H. C., Mann, S., Bazylinski, D. A., Lovley, D. R., Janasch, H. W. & Frankel, R. B. (1990) *Earth Planet. Sci. Lett.* **98**, 14–22.
13. Carr, M. H. (1996) in *Water on Mars* (Oxford Univ. Press, New York).
14. Malin, M. C. & Edgett, K. S. (2000) *Science* **288**, 2330–2335.
15. Clemett, S. J., Dulay, M. T., Gillette, J. S., Chillier, X. D. F., Mahajan, T. B. & Zare, R. N. (1998) *Faraday Discussion* **109**, 417–436.
16. Connerney, J. E. P., Acuna, M. H., Wasilewski, P. J., Ness, N. F., Rème, H., Mazelle, C., Vignes, D., Lin, R. P., Mitchell, D. L. K. & Cloutier, P. A. (1999) *Science* **284**, 794–798.
17. Gorby, Y. A., Beveridge, T. J. & Blakemore, R. P. (1988) *J. Bacteriol.* **170**, 834–841.
18. Kirschvink, J. L. (1982) *Earth Planet. Sci. Lett.* **59**, 388–392.
19. Guerinot, M. L. (1994) *Annu. Rev. Microbiol.* **48**, 743–772.
20. Braun, V., Hantke, K. & Koster, W. (1998) *Metal. Ions. in Biological Systems* **35**, 67–145.
21. Leshin, L. A. (2000) *Geophys. Res. Lett.* **27**, 2017–2020.
22. Meyer, C. (1998) *Mars Meteorite Compendium*. JSC. # 27672 (www-curator.jsc.nasa.gov/curator/antmet/mmc/mmc.htm).
23. Gooding, J. L., Wentworth, S. J. & Zolensky, M. E. (1991) *Meteoritics* **26**, 135–143.
24. Owen, T. (1992) in *Mars*, eds. Kieffer, H. H., Jakosky, B. M., Snyder, C. W. & Matthews, M. S. (Univ. of Arizona Press, Tucson, AZ), pp. 818–834.
25. Barth, C. A., Stewart, A. I. F., Bougher, S. W., Hunten, D. M., Bauer, S. J. & Nagy, A. F. (1992) in *Mars*, eds. Kieffer, H. H., Jakosky, B. M., Snyder, C. W. & Matthews, M. S. (Univ. of Arizona Press, Tucson), pp. 1054–1089.
26. Biemann, K., Oro, J., Toulmin, P., III, Orgel, L. E., Nier, A. O., Anderson, D. M., Simmonds, P. G., Flory, D., Diaz, A. V., Rushneck, D. R., *et al.* (1977) *J. Geophys. Res.* **82**, 4641–4658.
27. Benner, S. A., Devine, K. G., Matveeva, L. N. & Powell, D. H. (2000) *Proc. Nat. Acad. Sci. USA* **97**, 2425–2430. (First Published March 7, 2000; 10.1073/pnas.040539497)